



Enhancing performance of a linear dielectric based concentrating photovoltaic system using a reflective film along the edge



Hasan Baig^a, Nabin Sarmah^a, Daniel Chemisana^b, Joan Rosell^b, Tapas K. Mallick^{a,*}

^a Environment and Sustainability Institute, University of Exeter, Penryn, Cornwall TR10 9FE, UK

^b University of Lleida, Lleida, Spain

ARTICLE INFO

Article history:

Received 4 February 2014

Received in revised form

19 May 2014

Accepted 2 June 2014

Available online 22 July 2014

Keywords:

BIPV (Building Integrated Photovoltaics)

CPV

Non-uniformity

Reflective film

Modelling

FEA

ABSTRACT

In the present study, we model and analyse the performance of a dielectric based linear concentrating photovoltaic system using ray tracing and finite element methods. The results obtained are compared with the experiments. The system under study is a linear asymmetric CPC (Compound Parabolic Concentrator) designed to operate under extreme incident angles of 0° and 55° and have a geometrical concentration ratio of $2.8\times$. Initial experiments showed a maximum PR (power ratio) of 2.2 compared to a non concentrating counterpart. An improvement to this has been proposed and verified by adding a reflective film along the edges of the concentrator to capture the escaping rays and minimise optical losses. The addition of the reflective film changes the incoming distribution on the solar cell. Results show an increase of 16% in the average power output while using this reflective film. On including the thermal effects it was found that the overall benefit changes to about 6% while using a reflective film. Additionally, the effects of the non-uniformity of the incoming radiation are also analysed and reported for both the cases. It is found that adding the reflective film drops the maximum power at the output by only 0.5% due to the effect of non-uniformity.

© 2014 Elsevier Ltd. All rights reserved.

1. Introduction

PVs (photovoltaic devices) convert sunlight directly into electricity but have low efficiencies, typically in the range of 17–22%. These PV devices when used for grid connected electricity supply are subjected to further grid losses. BIPV (Building Integrated Photovoltaics) systems are gaining importance particularly because PV power is generated at the point of consumption reducing the supply losses and are very well integrated to the buildings architecture. However, this technology faces problems like low efficiency and high cost. Using Concentrating photovoltaic systems and coupling it with the building architecture could prove economical and sustainable solution. Building integrated Concentrating Photovoltaic (BiCPV) systems benefit from the concentrated sunlight and integrate well within the building architecture.

A CPC (Compound Parabolic Concentrator) designed for solar energy applications essentially consists of two different parabolic

reflectors. These parabolas reflect the incoming solar radiation and focus it on the absorber surface. In order to improve the efficiency of BIPV a concentrator could be integrated with the existing system [1–3], this would increase the incident solar radiation and reduce the area of the photovoltaic material needed, hence reducing the cost of the complete system. Low concentration compound parabolic reflectors, enable the capture of a large fraction of the diffuse solar radiation (in addition to the direct component) – especially relevant for northern European climatic conditions which experiences lesser sunny days. Depending on the location of the site the design of such systems changes considerably. Previous research showed that asymmetric compound parabolic PV concentrator significantly increased its power output compared to the flat PV system and suitable for building façade or window integration in the UK. Several designs of CPC for different absorbers have been presented [4–6] and detailed parametric and experimental analyses of optics and heat transfer have been undertaken. Studies [7] show that the use of CPC can enhance the efficiency of PV system by more than 60% to that compared with a standalone PV system. Low cost dielectric materials have been utilised in concentrators [8] termed as PRIDE (Photovoltaic Facades of Reduced Costs Incorporating Devices with Optically Concentrating Elements) technology incorporating 3 and 9 mm wide single crystal silicon solar cells.

* Corresponding author. Tel.: +44 (0) 1326 259465.

E-mail addresses: mail2baig@gmail.com (H. Baig), t.k.mallick@exeter.ac.uk (T.K. Mallick).

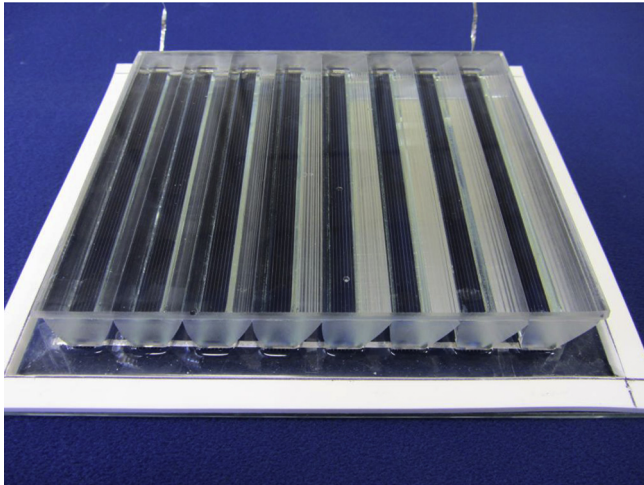


Fig. 1. Sample of the concentrator element made using polyurethane.

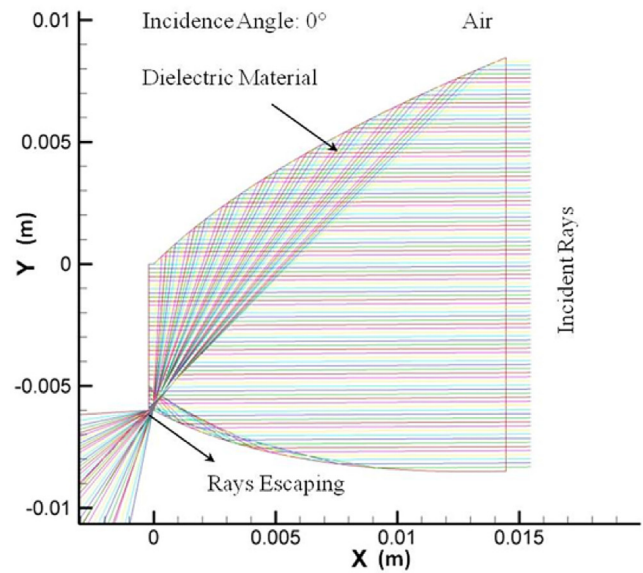
Results showed excellent power output compared to a similar non-concentrating system when it was characterised both indoors using a flash and continuous solar simulator. A second generation PRIDE concentrating system was developed to incorporate 6 mm ‘Saturn’ solar cells because of the problems in the optical system in the previous generation [8]. Using injection moulding process the optical concentrator was made and a 3 kWp was built and tested experimentally. A power ratio of 2.01 was found.

In the present study, a third generation of similar concentrator with an added reflective film on the concentrator edges is presented. Recently, a procedure to carry out a detailed analysis of such a system was presented [9]. However, there were some shortcomings in the modelled results. The modelling parameters were essentially taken from a published data. In the present study the modelling parameters have been exclusively evaluated for the solar cell under study. Using the new model parameters, the system is

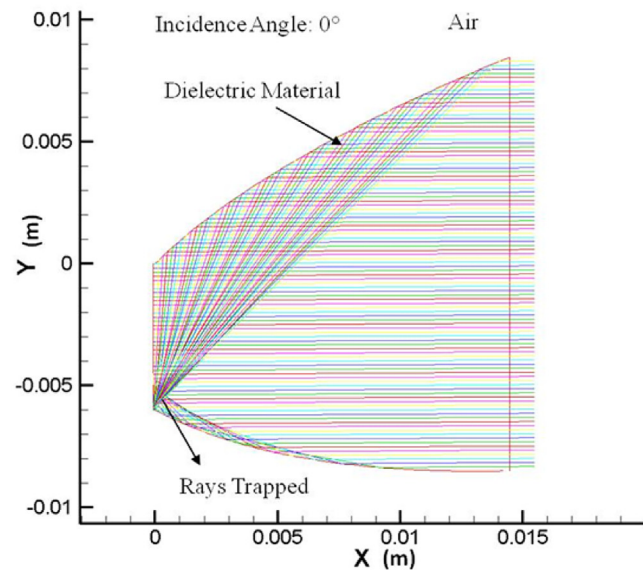
analysed to understand the benefit of adding a reflective film at the edges of the concentrating element. Using Ray trace method the optical analysis of the concentrating element is carried out. Based on the optical results the electrical and the thermal performance of the solar cell is modelled using finite element method. Finally, the overall system outputs are compared for the case of a CPV unit with and without a reflective film.

2. Linear concentrating photovoltaic system

The system as shown in Fig. 1 is a linear concentrating photovoltaic system essentially consisting of a linear (line-axis)



(a) No Reflective Film



(b) With Reflective Film

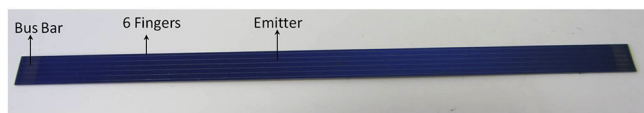


Fig. 2. Solar Cell used in the system.

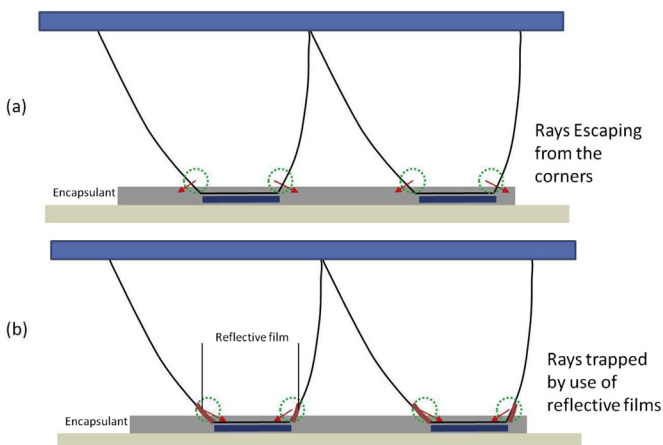


Fig. 3. Schematic of the system while using a reflective film along its edges.

Fig. 4. Schematic ray-trace diagram of the DiACPC-55 with 100 representative rays when used without and with a reflective film.

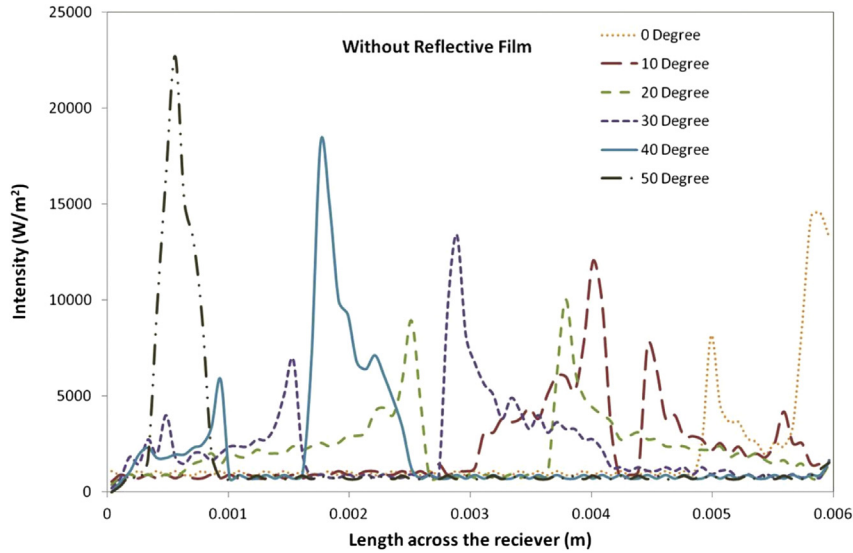


Fig. 5. Energy flux distribution on receiver without reflective film on the edges.

concentrator element attached to a solar cell using an encapsulation material and placed between two glass sheets. The concentrating element is a dielectric asymmetric compound parabolic concentrator with acceptance half angles (0° & 55°). The concentrator design is two-dimensional which means it would experience similar illumination profile along its length. The main application of the system is to serve as a double glazed building integrated photovoltaic system employing concentrating technology [9]. Clear polyurethane material crystal-clear 200[®] [10] due to its good transmission and dielectric properties is used to prepare the concentrating element. The concentrator material is resistant to humidity and several other solvents. Sylgard-184 [11] is used as an encapsulation material, it not only helps to prevent the solar cell from weathering, but also acts as an adhesive between the concentrator and the solar cell. The Laser Grooved Buried Contact solar cells used in this system are 6 mm wide and 116 mm long and have two bus bars towards its corners each 2.5 mm wide. The cell has six grid fingers having a width of 35 μm , spaced 965 μm apart as

shown in Fig. 2. The remaining area on the top surface is known as the emitter (blue colour).

The following steps are adopted to prepare the array of concentrating elements.

1. The casts are cleaned and dried.
2. The polyurethane material is prepared according to the requirements and poured in these castings.
3. A curing process follows this.
4. Using thin tin-plated copper strips the solar cells are soldered in series.
5. The solar cells are fixed on a glass plate using a glue material.
6. The encapsulant is prepared and poured all over the solar cells until it distributed smoothly over the surface and left to dry overnight.

Different natural phenomena occur in the CPV system [9], the upper layer which is usually made of glass transmits light to the

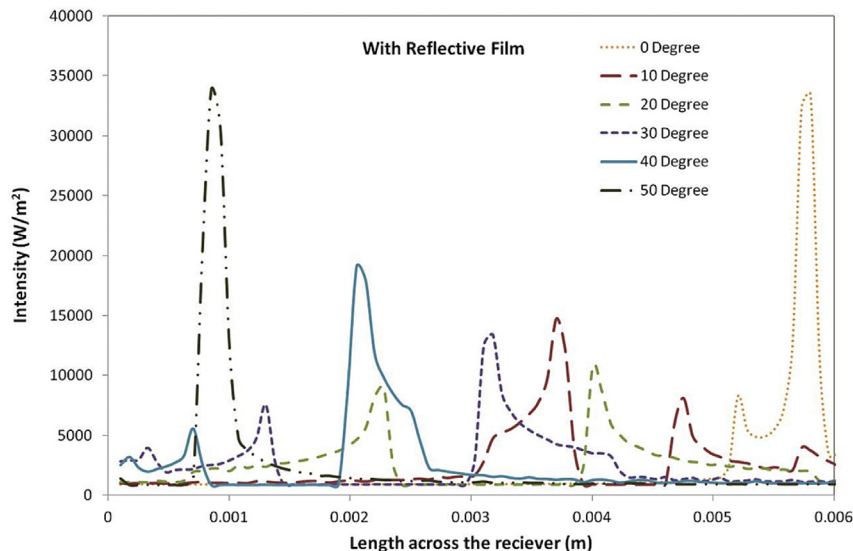


Fig. 6. Energy flux distribution on receiver with reflective film on the edges.

dielectric concentrator which further concentrates the light on the cell by total internal reflection. The encapsulation layer between the cell and the concentrator reduces the intensity by 5–10%. Silicon elastomer having the same refractive index (1.5) is used to encapsulate the solar cell and to bind the concentrators on top of the solar cells in proper alignment. The solar cell generates electricity while receiving the irradiation. Only a part of the total energy is converted to electricity while the rest is dissipated as heat to the adjoining glass layers and the air gaps. Some of the light escapes through the gaps and is transmitted which helps for day lighting purposes. One of its main features is that it is transparent and refracts all the light entering the aperture via total internal reflection. It has good transmission properties and excellent strength and rigidity to retain the shape of the complex profile.

3. Optical analysis

The optical model was based on the refraction laws where a source of light with desired intensity impinges on the concentrator and the output along the absorber surface is estimated. The optical efficiency of the CPC is obtained for different incident angles of the incident rays. For each incident angle, an optical simulation is carried out determining the energy of the incident rays reaching the solar cells after going through the refractive element.

Only an optical analysis of the system has been presented earlier [12] highlighting the procedure and comparing the results obtained for three DiACPC (Dielectric Asymmetric Compound Parabolic Concentrators) with different acceptance angles. During manufacture of the system a key defect was causing the rays to escape from the edges of the concentrator. The spreading of the encapsulant layer around the borders of the concentrator was causing the rays near the borders to escape out because of similar refractive index as shown in Fig. 3(a). During the manufacture process it is a normal practice to use an encapsulant material to act as an adhesive between the concentrator and the solar cell and at the same time protect the solar cell from weathering. In order to reduce these losses a reflective film can be added along the boundaries of the concentrator upto the height of the adjoining encapsulant layer as shown in Fig. 3(b). This reflective film redirects the escaping rays towards the solar cell.

In order to identify these losses in the real situation, the optical analysis is carried out for the DiACPC-55 while considering additional encapsulant material around the edges so that the light escapes through refraction around the concentrator edges.

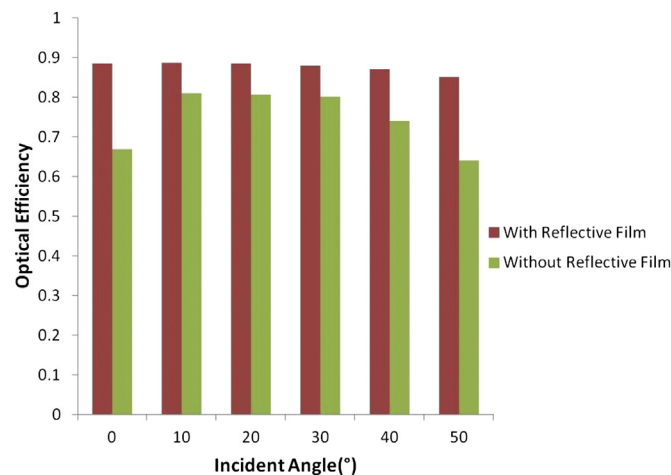


Fig. 7. Comparison of the optical efficiency of the system at different incident angles.

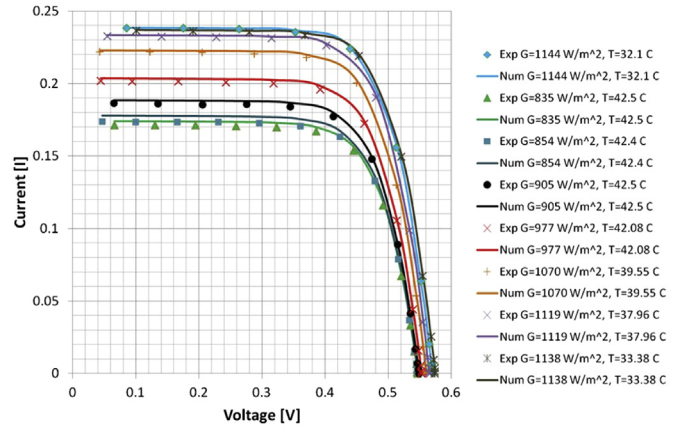


Fig. 8. Comparison of model simulated and experimentally obtained I–V characteristics for different levels of solar radiation and operating temperature.

A schematic ray–trace diagram of the DiACPC-55 with 100 representative rays is shown in Fig. 4. The light rays entering the concentrator undergo four possible behaviours while entering the concentrator.

1. Rays reach the solar cell surface directly without any reflection
2. Rays reach the solar cell surface by one or more reflection
3. Rays escape the concentrator edges due to the presence of the encapsulant material
4. Reflected back by the metallisation present on the solar cell or due to multiple reflections occurring in the concentrator

3.1. Energy flux distributions at the receiver

The optical analysis is performed mainly to determine the light intensity and its distribution on the exit aperture of the concentrating element. These parameters determine the amount of power produced by the solar cell attached to the concentrator. A homogeneous flux distribution is always desirable for attaining higher electrical efficiency and increasing the reliability of the solar cell device however the concentrating light is found to have a non-uniform distribution. This non-uniformity can have a parasitic effect on the performance of the system [13]. Figs. 5 and 6 represent the energy flux distributions at the receiver under a direct insolation of 1000 W/m² when the system is operating with and without

Table 1
Solar cell parameters.

Cell parameters	Values
Cell width	6 mm
Cell length	115 mm
Busbar width	2.5 mm
Finger width	35 μm
Emitter sheet resistance	100 Ω/□
Finger resistance per unit length	0.3 Ω/cm
<i>Operating conditions</i>	
Illumination intensity range G	835–1144 W/m ²
Temperature range T	32–42.5 °C
<i>Diode equation parameters</i>	
Constant j ₁	0.423364826 AW ⁻¹
Constant j ₂	–2551484.076 Am ⁻² .K ⁻³
Constant j ₃	–183.38 Am ⁻² .V ⁻¹
Ideality factor n	1.33
E _g	1.124 eV
k _B	1.380 × 10 ⁻²³ J.K ⁻¹
q _e	1.602 × 10 ⁻¹⁹ C

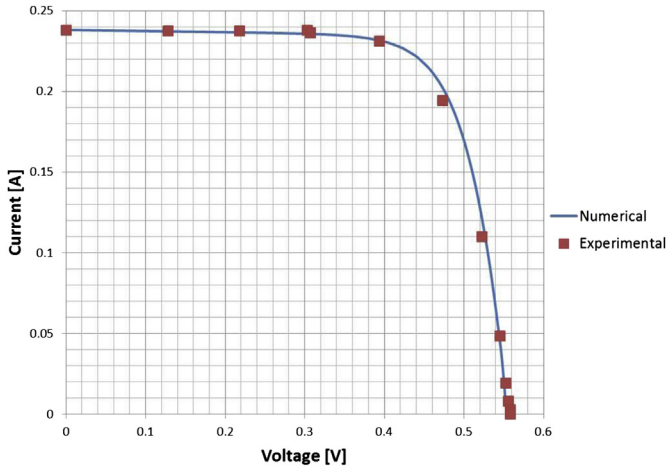


Fig. 9. Experimental and finite element simulated I - V characteristics of a solar cell under uniform illumination 1141 W/m^2 and temperature of 314 K .

a reflective film. The figures show the variation of the light intensity falling on the solar cell at different angles of incidence. It may be seen that the energy distribution changes both its peak and the location for different incident angles for the two cases.

In the case of the concentrator, with reflective film the peak values can be seen to reach 34 suns at incident angles of 0 and 50° , which represent extreme angles. However in the case without

reflective film, the peaks go only up to 24 and 15 suns for extreme angles of 0 and 50° . The peaks are observed to be sharp close to the acceptance angles because of the reflections due to the parabolic surfaces. The energy flux at the receiver is calculated from Eq. (1) where I_{rec} is the intensity at the receiver (W/m^2) as indicated previously in Ref. [12].

$$I_{\text{rec}} = I_0 - \sum_{i=1}^m (\tau_g I_i + \tau_d I_i + j\rho I_i) \quad (1)$$

The optical efficiency may be defined as the ratio of solar radiation at the absorber surface i.e., the solar cell to the incoming radiation at its aperture. In the present analysis the optical efficiency is evaluated using the Eq. (2). The average illumination (G_{avg}) is calculated for each incident angle. The value of G_{incident} is taken as 1000 W/m^2 in our analysis. Fig. 7 shows the variation of the optical efficiency with respect to the incidence angle.

$$\eta_{\text{opt}} = \frac{G_{\text{avg}} * A_{\text{receiver}}}{G_{\text{incident}} * A_{\text{aperture}}} \quad (2)$$

It may be clearly noted that the optical efficiency in the case of the system with reflective film is higher than the optical efficiency of the system without the reflective film. The figure quantifies the losses occurring in the system by the escaping light. The impact of these phenomena is now studied on the overall performance of the solar cell using the finite element method which is detailed in the following sections. The output illumination intensity is utilised to determine the electrical performance of the system.

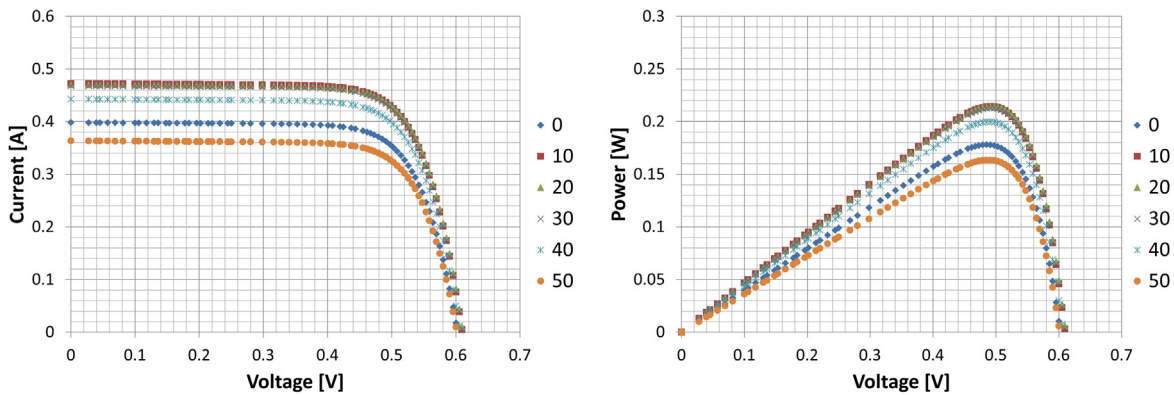


Fig. 10. Electrical output at different incidence angles for system without reflective film.

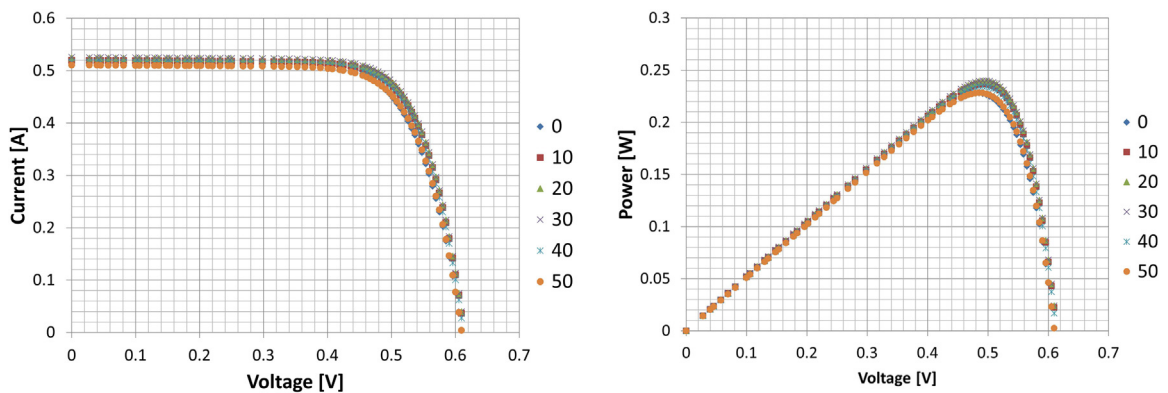


Fig. 11. Electrical output at different incidence angles for system with reflective film.

4. Electrical analysis & performance

The electrical analysis is based on the one diode model and is performed in accordance to the method reported elsewhere [9]. Considerable difference was found between modelled and experimental results previously, and suggestions were made to reevaluate the solar cell constants. We have covered this gap in the present study and characterised the solar cells according to the procedure described in Ref. [6] and extracted constants specific to this solar cell. The solar cell used and the conditions applied in the present

study are different to that reported [6], however similar experimental procedure has been used. The test conditions and the parameters extracted are presented in Fig. 8. In order to perform the electrical analysis of the solar cell under non-uniform illumination, it is important to first evaluate the intensity distribution at different incident angles. In the previous section the intensity distributions were evaluated for both the cases of with and without reflective films.

The use of COMSOL Multiphysics software is made in our study to obtain the solution. The continuity equation as shown in Eq. (3) is

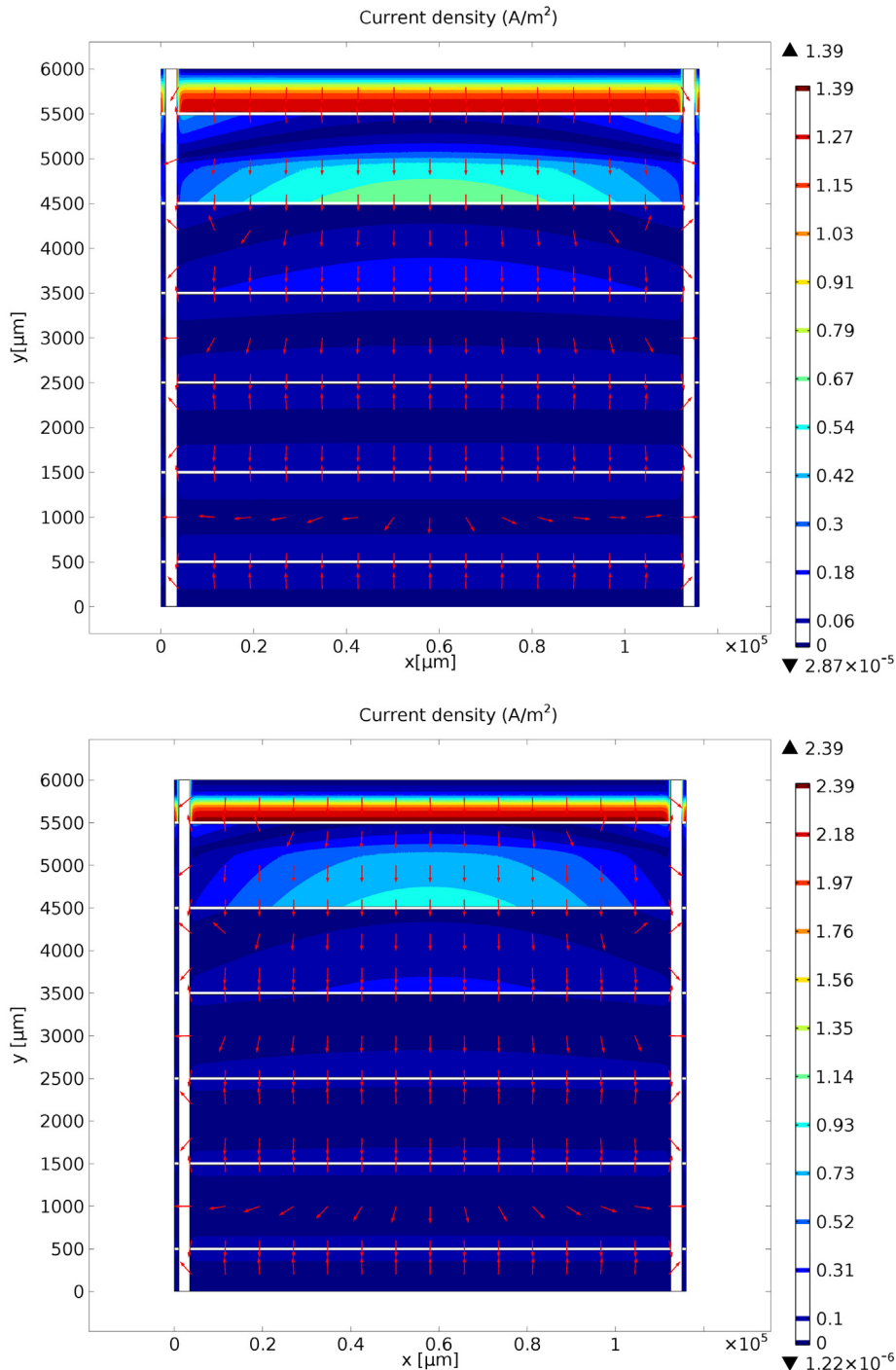


Fig. 12. Current generated in the solar cell for a system with and without reflective film at I_{sc} .



Fig. 13. Experimental setup showing the solar simulator and the tilted module.

solved to determine the voltage and the effective current density distribution on the surface the solar cell subjected to non-uniform illumination for both the cases.

$$-\nabla \cdot (\sigma \nabla V - J^e) = Q \quad (3)$$

where V is the electric potential, J^e is the current density and Q represents the current generated or the source term and σ is the conductivity of the material. The current generated in the illuminated emitter region Q_e and in the dark region Q_d may be expressed as

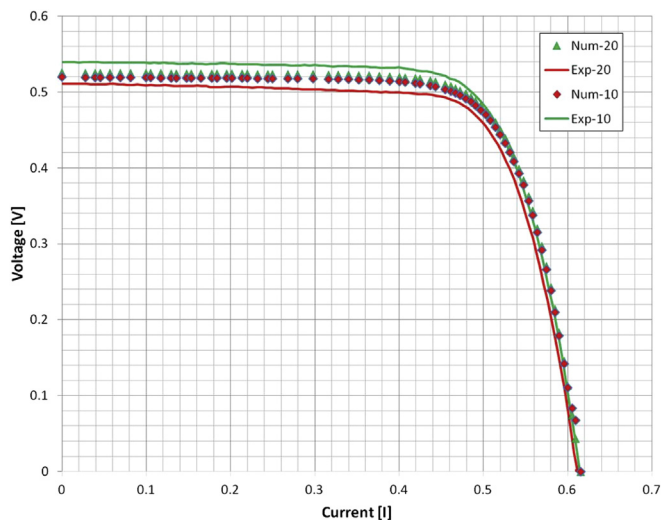


Fig. 14. Comparison of experimental and numerical results for the system with reflective film at 10° and 30° incident angle.

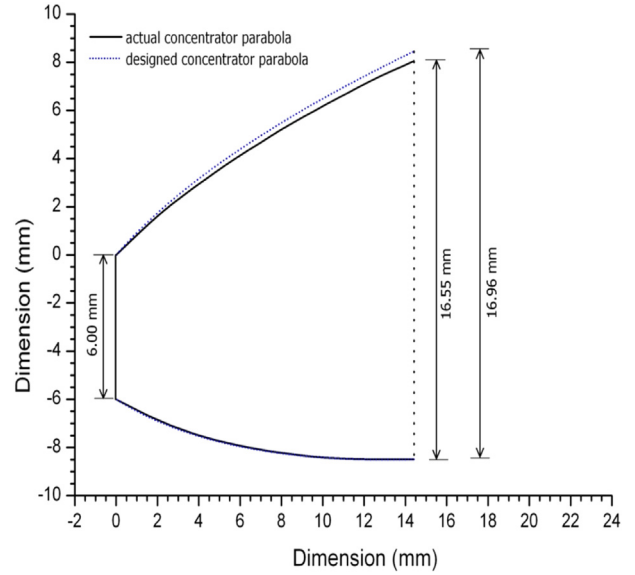


Fig. 15. Manufacturing errors.

$$Q_e = j_1 G + j_2 T^3 \exp \left[\frac{-E_g}{k_B T} \right] \left(\exp \left[\frac{V_j}{n_1 V_T} \right] - 1 \right) + j_3 V_j \quad (4)$$

$$Q_d = j_2 T^3 \exp \left[\frac{-E_g}{k_B T} \right] \left(\exp \left[\frac{V_j}{n_1 V_T} \right] - 1 \right) + j_3 V_j \quad (5)$$

where j_1, j_2, j_3 are constants, E_g represents the band gap energy, k_B is the Boltzmann constant, V_T is the thermodynamic voltage, V_j is the junction potential and n is the ideality factor. The presence of non-uniformity and modification in the flux intensity by concentration changes all the parameters with respect to the spatial location making it as $G(x, y)$ [W/m^2]. The photovoltaic efficiency may be defined as shown in Eq (6). Where the product $G \times A$ is the power incident on the cell, and can be obtained using ray tracing techniques. I_{sc} is the short circuit current, V_{oc} is the open circuit voltage and FF represents the solar cell fill factor.

$$\eta = \frac{I_{sc} V_{oc} FF}{GA} \quad (6)$$

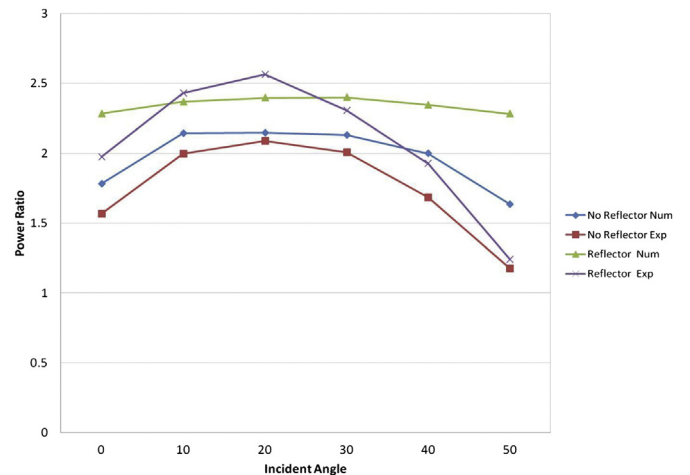


Fig. 16. Comparison of power ratios for system with and without reflective film.

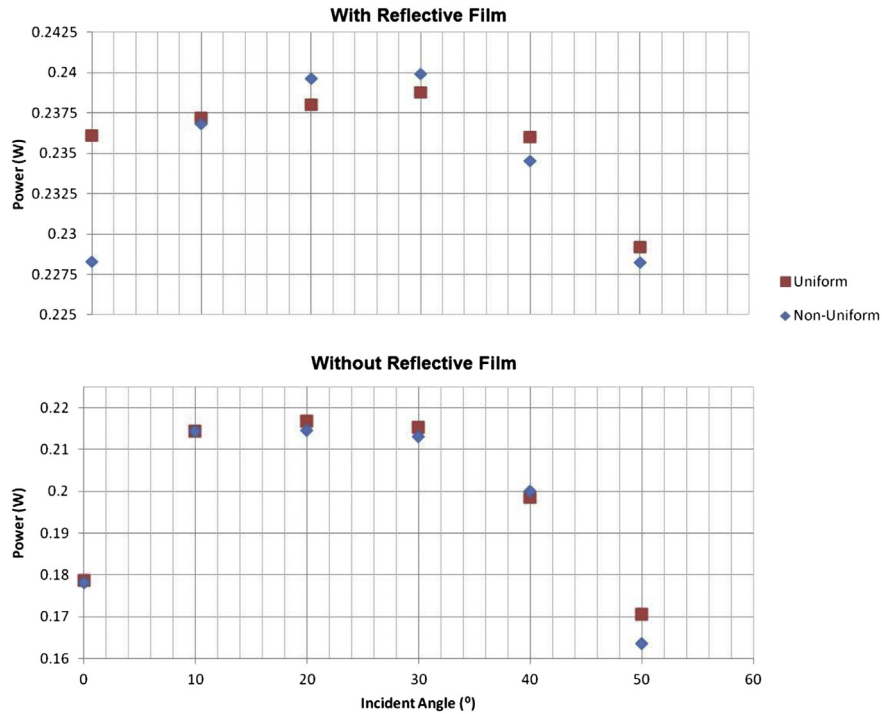


Fig. 17. Maximum power output in both the systems under uniform and non-uniform conditions.

It is very important to validate the numerical model before its application. To do so, the $I-V$ characteristics of the solar cell are evaluated under different illumination and temperature conditions. In the present study we have changed the illumination between 835 and 1144 W/m^2 curve fitting is performed on this experimentally evaluated data using statistical techniques according to the procedure highlighted in Ref. [6]. The comparison of the simulated values of current with the experimental data is shown in Fig. 8. The parameters j_1 , j_2 and j_3 extracted from this statistical fitting operation are listed below in Table 1.

4.1. Validation of results

In order to verify the accuracy of the model finite element modelling of the solar cell was carried out at different operating

condition. Details of the modelling procedure, boundary conditions employed may be found here [9]. Improved model is uses the new fitted parameters as shown in Table 1. An example of such analysis is compared with the experimental results for uniform illumination of 1141 W/m^2 and temperature of 314 K and is shown in Fig. 9. It may be seen clearly that the numerical model is accurate with less than $\pm 2\%$ error.

4.2. Analysis of angular performance

To understand the overall energy production of the system it needs to be analysed at different angles representing the variable sun positions throughout the day. In the previous section, the optical analysis is carried out at different incident angles. Based on the illumination profile output obtained from this optical analysis, the

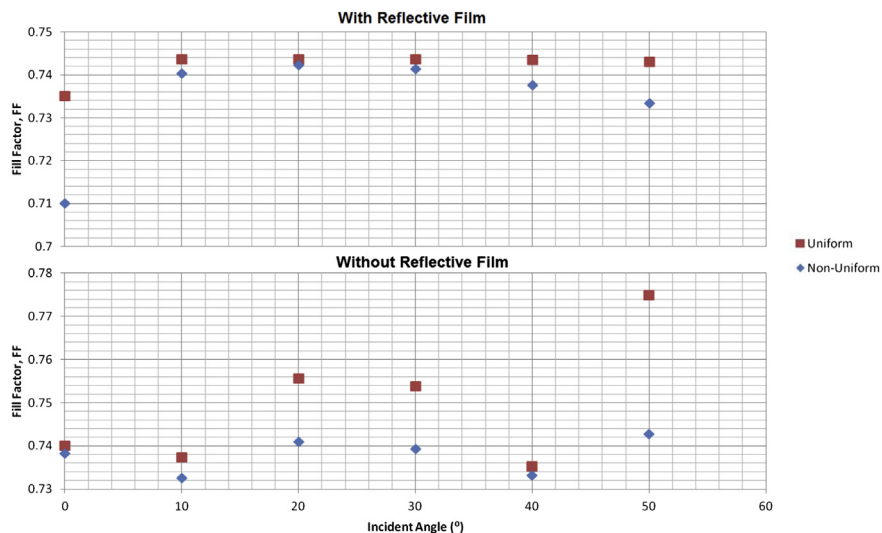


Fig. 18. Comparison of FF under uniform and non-uniform illumination conditions for both the systems.

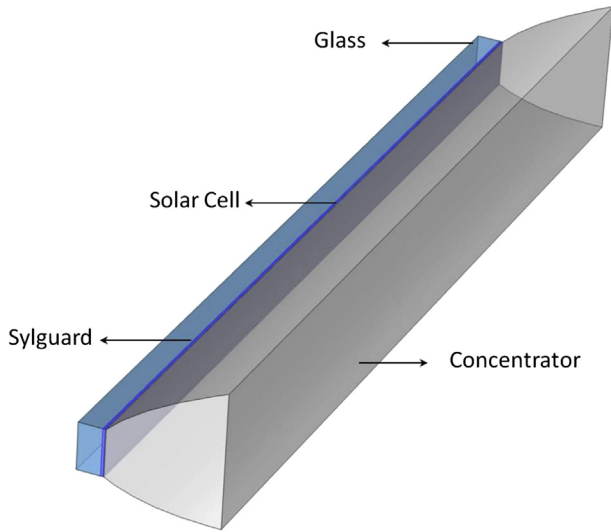


Fig. 19. Geometry used for the thermal analysis.

electrical performance of the solar cell was simulated for the case with and without reflective film. The $I-V$ characteristics obtained are shown in Figs. 10 and 11. The behaviour of the solar cell is found to change substantially when comparing both the scenarios at different incidence angles. A clear increase in the electrical output may be seen in the results by the use of reflective film. As shown in Fig. 11, a consistent output is seen across different incidence angles. A maximum short circuit of 0.52168 A is observed at 0° incidence angle in the case with reflective film, as compared to 0.39308 A observed in the case without the reflective film.

This substantially boosts the power output; however the important point to consider is that these simulations are carried out a constant cell temperature in both the cases which might not be true in realistic conditions. The effect of temperature on the output and the comparison of important parameters obtained from the $I-V$ curves are discussed in detail in the next few sections. The incoming illumination profile directs the current generation on the

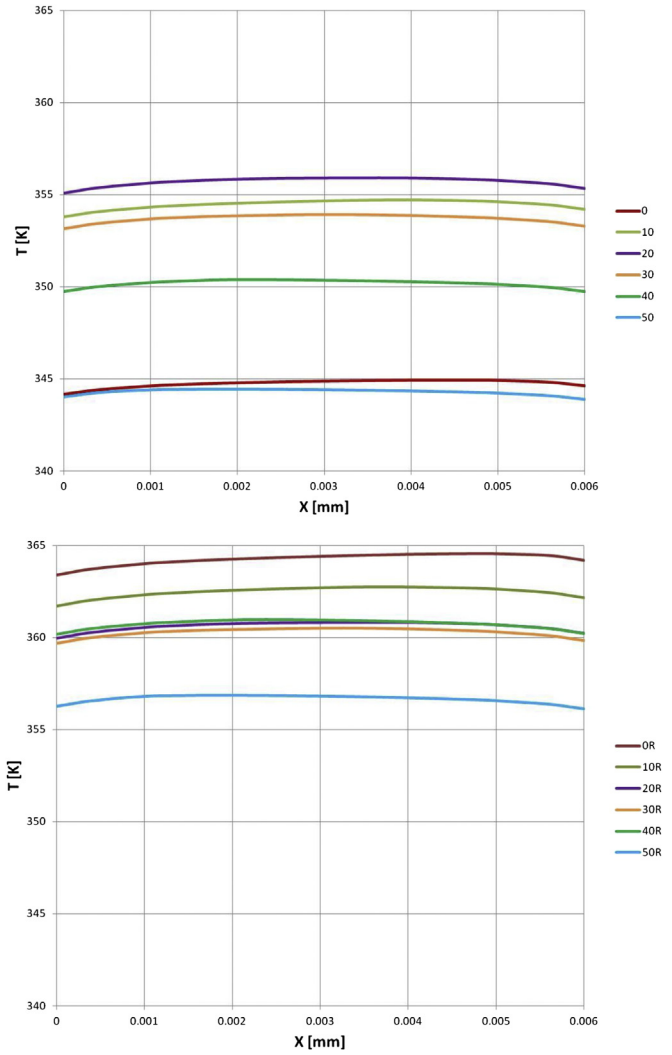


Fig. 21. Comparison of temperature along solar cells with and without reflector.

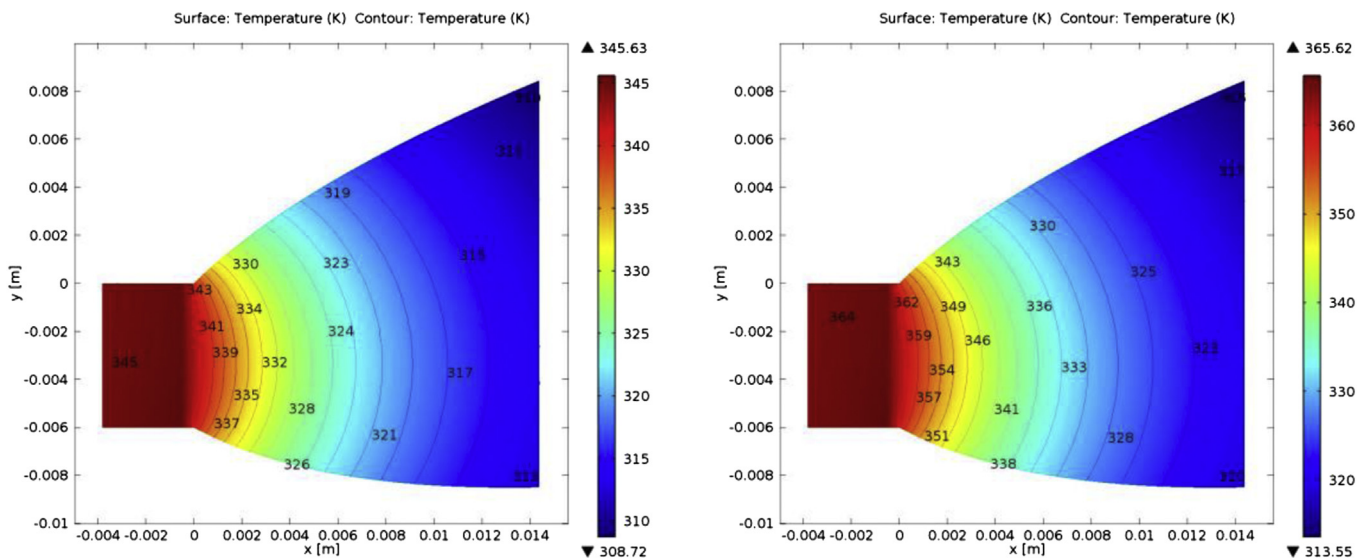


Fig. 20. Temperature contours of the CPV system with and without reflector at 0° incidence angle.

solar cell, with higher densities being generated at the points receiving peak intensities. This imbalance in current generation causes a local resistance adding up the existing series resistance of the solar cell. Additionally, it also causes a non-uniform solar cell temperature. Fig. 12 shows the current density at short circuit conditions in the solar cell when placed under the CPC with and without the reflective film for 0° incident angle. As expected, the current in the solar cell is greater for the case with the reflective film. The arrows show the current density generation and its direction to the fingers and the bus bars. These plots are made to visualise the impact of the non-uniform illumination and not for making any analysis. It may be seen clearly that the current generation at points of higher illumination intensities is higher. These currents in the emitter region are accumulated at the Busbar while flowing through the fingers on the solar cell.

Experiments were carried out to see the impact of introducing the reflective film in the CPV system. The use of a special setup to change the angular position of the concentrator unit was utilised. The setup consisted of a base plate which may be inclined at any desired inclination with respect to the incoming illumination, in one dimension. The $I-V$ characteristics were recorded at different angles using an experimental setup which consists of a solar

simulator, an $I-V$ tracer and an inclining bench. The solar simulator from Wacom having AAA rating and 2% spatial non-uniformity was used to carry out the experiments as shown in Fig. 13.

The illumination intensity distribution obtained while carrying the optical analysis of the system is used to carry out the electrical analysis of the single concentrator unit at different angles. A sample result at 30° incident angle is shown in Fig. 14 for a system with the reflective film.

Slight deviations are found while comparing with experiments, which are predominantly due to the manufacturing defects of the concentrator. Fig. 15 compares the designed geometry with the manufactured product. The deviations of the numerical results at these points are attributed to the losses occurring at the edges of the concentrator due to the accumulation of encapsulation layers and are relative to the optical efficiencies.

To measure the overall performance of the system the parameter PR (Power Ratio) is used in our study. The power ratio represents the ratio of the power output of the unit system to the power obtained by a bare cell. The power ratio was evaluated for different angles and is presented in Fig. 16. A maximum power ratio of 2.56 was found in our study when comparing the electrical output of the concentrator unit with the reflective film compared to the earlier

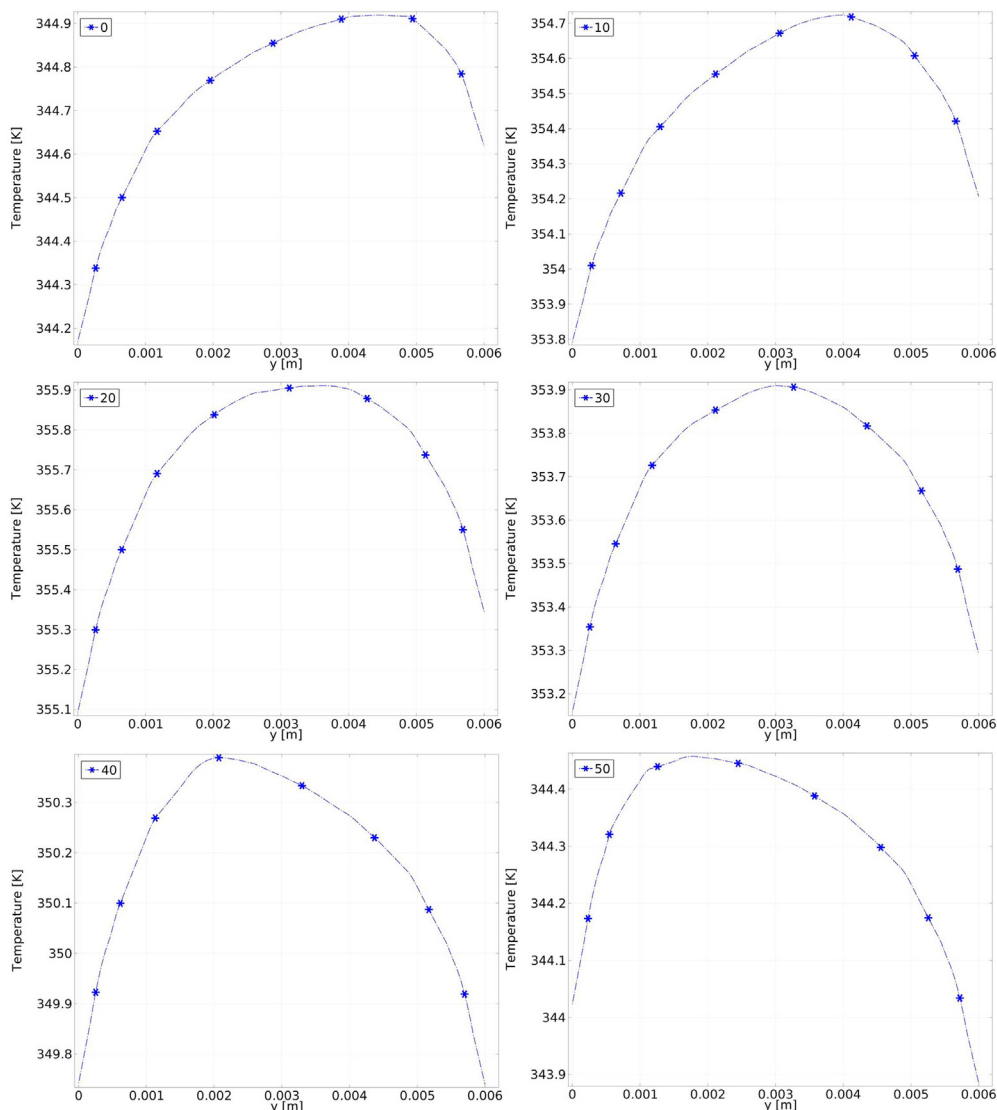


Fig. 22. Temperature profiles across the solar cells without reflector.

power ratio of 2.2 without a reflective film. With increasing incidence angles the power ratio drops due to the higher optical losses and the decrease in the optical efficiency of the system. The difference between the experimental and numerical results is primarily due to the manufacturing defects of the system and is in line with the optical efficiencies of the system. When compared to a flat PV panel having a similar area as that of the input face of the concentrator, the system generates lesser power due to the optical losses. A PR of 2.2 without the reflective film indicates optical losses of 21.5%. The CPV system uses 64% less solar cell than a flat PV panel, which means the cost of CPV system is 50% (assuming negligible cost of about 14% for making the concentrator). Which means the cost per unit output is 39.25% less than the standard PV module. While using a reflective film the optical losses are reduced considerably, indicating the system to cost 45% less than the PV panel.

4.3. Effect of non-uniformity

The non-uniform illumination distribution over the solar cell usually creates hotspots on the solar cell and tends to reduce its

durability [13]. It is always desired by the CPV system designers to have a lower degree of non-uniformity for increased reliability of the system. Quantifying these losses helps the solar cell designer to prepare the metallisation accordingly and helps in the proper system sizing. A recent study [14] also demonstrated non-uniformity could prove beneficial in increasing the electrical power output of the solar cell when associated with a particular temperature profile. In the present study, we analyse the impact of the change in the illumination intensity distribution under different angles of incidence for both the systems with and without the reflective film. A parametric analysis is carried out while biasing the cell to evaluate the $I-V$ curve of the cells subjected to both uniform and non-uniform illumination patterns. Applying bias on the cell in small increments, the output power and current are modelled for both uniform and non-uniform illumination conditions. In both cases the total illumination on the cell is identical and a constant temperature is maintained across the solar cell. Fig. 17 shows the comparison of the maximum power obtained under uniform and non-uniform illumination conditions. It may be seen in both the cases that non-uniformity tends to have both beneficial and detrimental effect

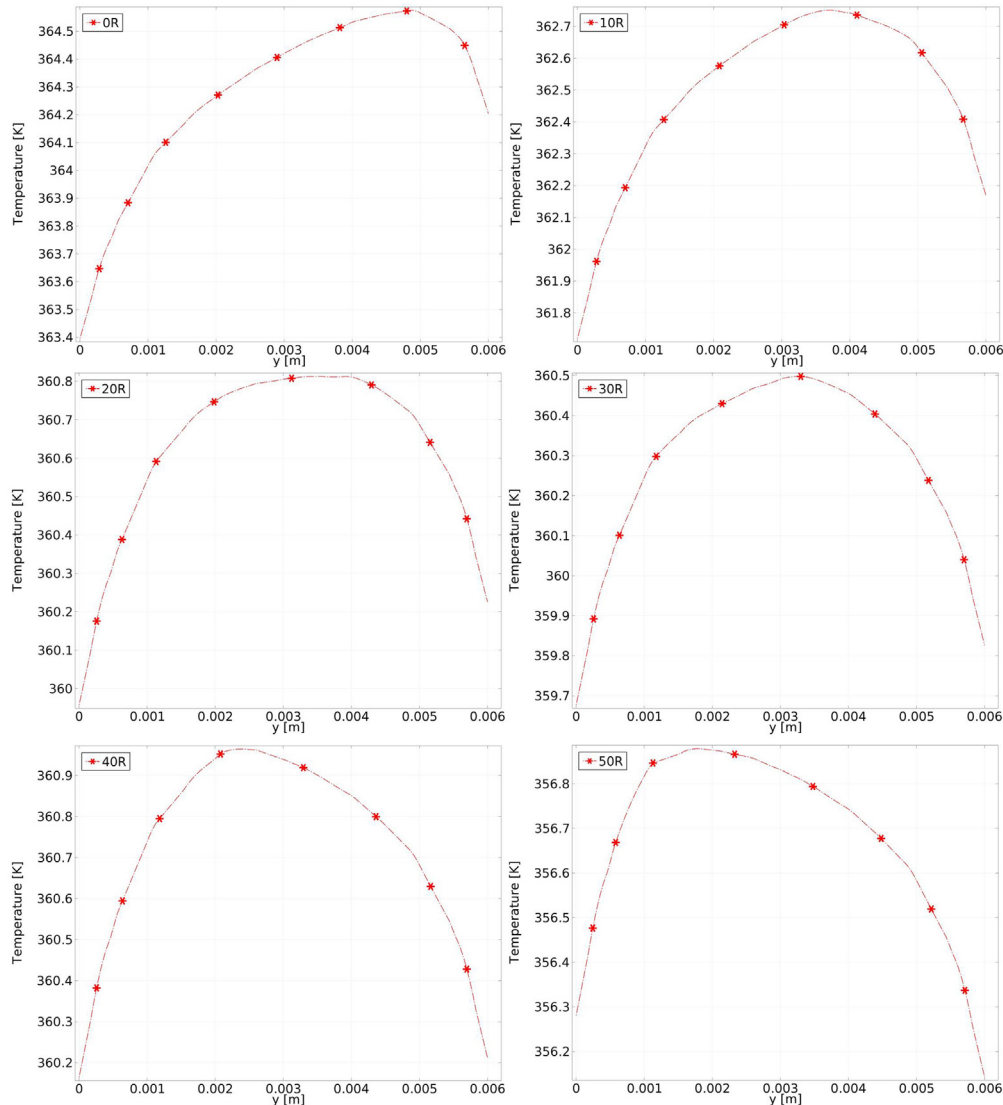


Fig. 23. Temperature profiles across the solar cells with reflector.

on the overall power production. In the case with no reflective film we can observe that the difference between modelled outputs is very much less. On averaging the output power at various angles it was found that the overall power decreases due to non-uniformity by 0.94%. In the case with the reflective film it may be seen that at incident angles of 20 and 30°, the output power exceeds the power obtained under uniform conditions. Overall, on averaging the impact at different angles the output power was found to drop by only 0.5% due to non-uniformity. Fig. 18 shows the simulated Fill Factor values under both uniform and non-uniform illumination conditions. A drop in the fill factor values may be consistently seen potentially due to the effect of non-uniformity. The magnitude of this drop is 1.53% and 1.07% in the case of system with and without the reflective film. Other important notable effects of non-uniformity are in the open circuit voltage. The non-uniformity of illumination tends to generate small local currents at operating conditions close to the open circuit voltage. These small currents cause a gradient in the voltage across the solar cell.

5. Thermal analysis

The temperature of the solar cell is very important factor affecting the overall energy output of the CPV system. The V_{oc} of the solar cell tends to drop quickly by the increase in its temperature and so the fill factor and the maximum power output drops immediately. Recent study [14] has also shown that the distribution of temperature also has affects the overall performance of the solar cell and if tuned properly it can actually help in improving the performance of the system. The operating temperature of the solar cell is evaluated under steady state conditions performing a heat transfer analysis of the system using finite element method. The geometry of the system being analysed is shown in Fig. 19. A mesh independency test is carried out to confirm the accuracy of the solution.

The boundary conditions applied to the system include, a convective heat transfer condition at the top and bottom surface of the system with $h = 10 \text{ W/m}^2 \cdot \text{K}$ on the exterior surfaces of the system and a convective heat transfer coefficient of $h = 7 \text{ W/m}^2 \cdot \text{K}$

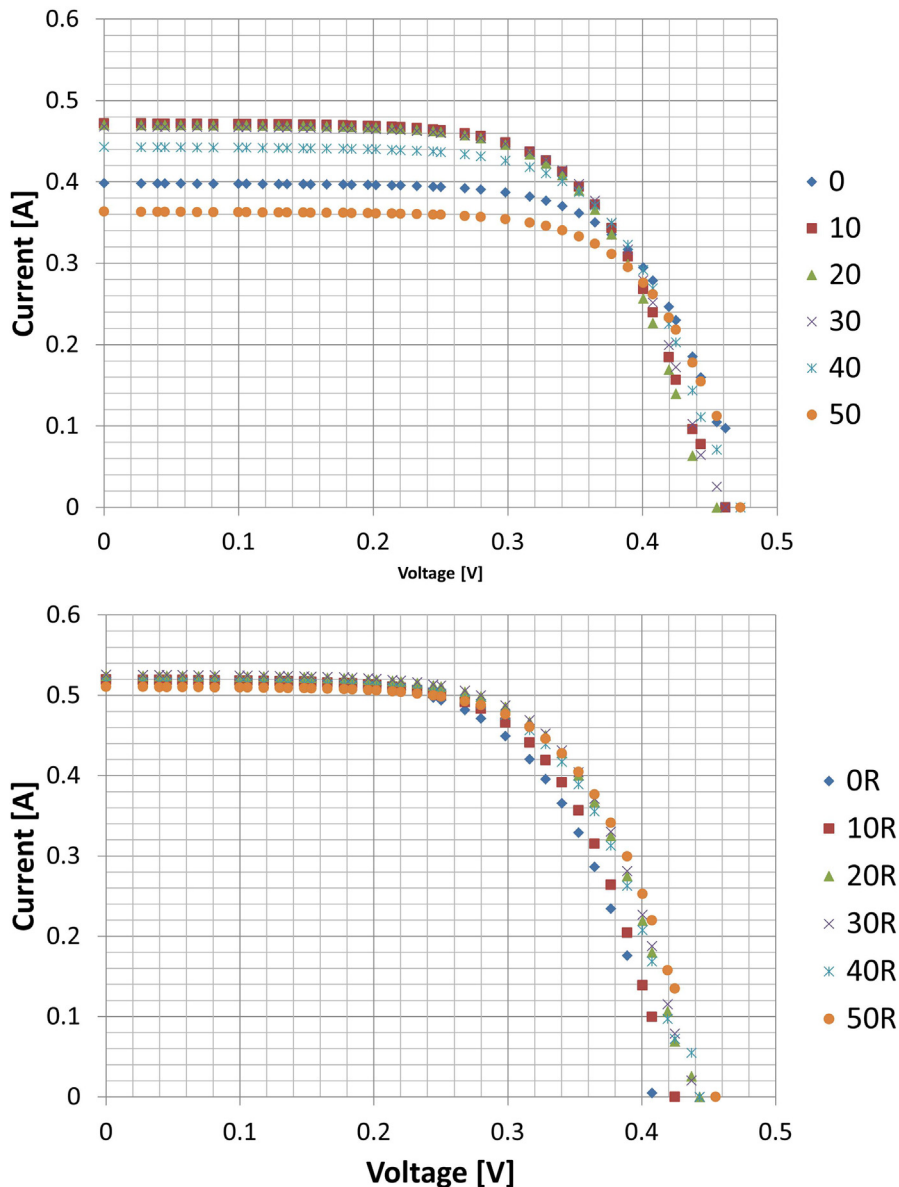


Fig. 24. I–V characteristics of the system under operating temperature profiles.

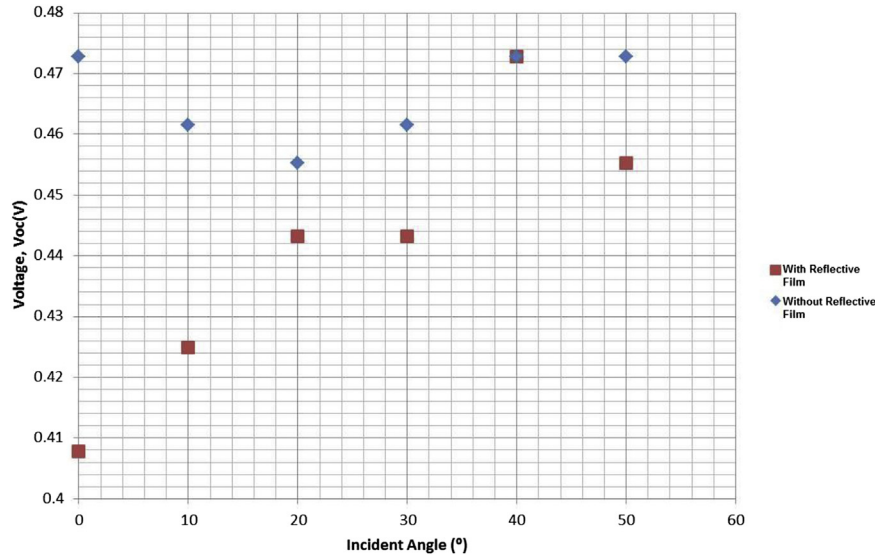


Fig. 25. Variation of the V_{oc} with and without the reflective film.

on the interior surfaces further details on these and the thermo physical properties used can be found [9]. The heat generated from the solar cell whilst converting the available irradiation to the electrical energy is considered as a heat flux condition at the base of the solar cell surface. The use of symmetry boundary condition (adiabatic boundary) was made towards the side edges of the glass plate. A typical result at 0° incidence for the case without and with reflective film can be seen in Fig. 20, the temperature distribution varies in the range of 308–345 K in the system without the reflective film and 313–365 K in the case with the reflective film.

The heat transfer analysis is carried out for different angular positions. The temperature profiles at the solar cell surface found with and without a reflective film are shown in Figs. 21–23. It was found that the temperature across the solar cell changes drastically by the use of the reflective film. The highest temperature of 364 K is seen in the case with the reflective film at 0° incident angle compared to 343 K seen in the unit without reflective film. Similar increase is visible at all other angles of incidence due to the use of

the reflective film compared to its counterpart without reflective film. Using the temperature distributions obtained from the thermal analysis, the $T(y)$ is used to perform the electrical analysis whose results are highlighted in the next section.

6. System output

The current study was carried essentially to predict the impact of placing the reflective film along the edges of the CPC and see the effects. As can be seen in the previous section, there is a considerable increase in the flux incident on the solar cell due to placement of this reflective film which has also a detrimental effect of raising the solar cell temperature. The temperature profiles obtained at different incident angles under both the scenarios of our study are now used to evaluate the steady state electrical performance of the system. Using the obtained temperature profiles the $I-V$ characteristics are evaluated as shown in Fig. 24. A clear drop in the V_{oc} values is visible in both the scenarios depending on the

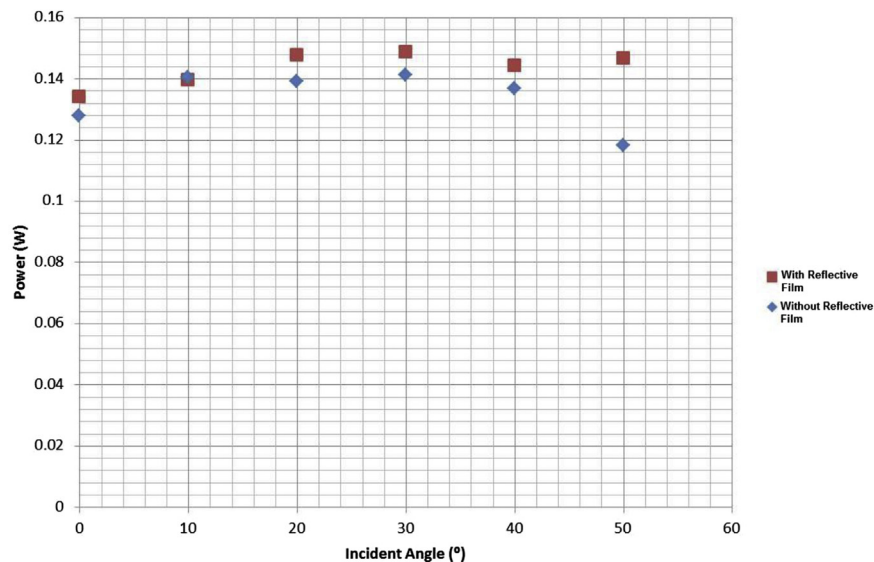


Fig. 26. Maximum power produced in the CPV system with and without the reflective film.

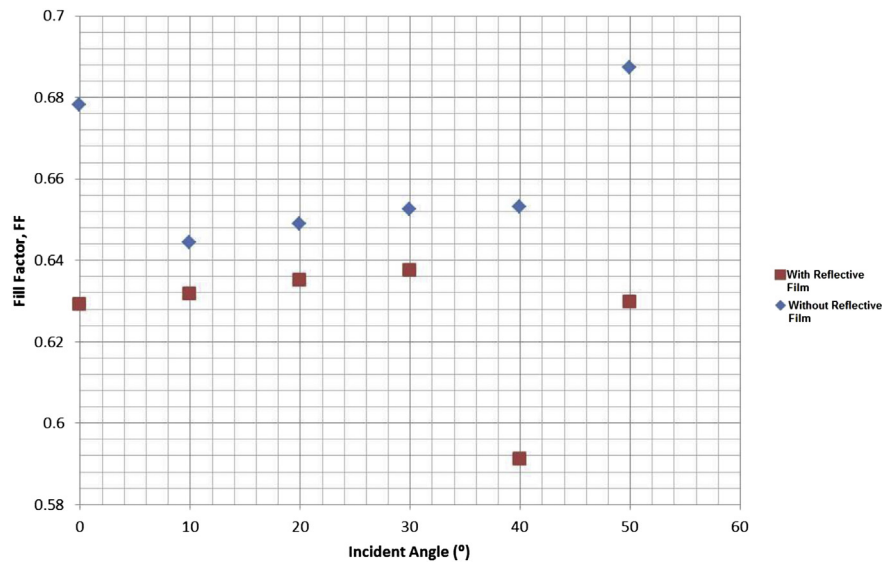


Fig. 27. Variation of the fill factor with and without the reflective film.

Table 2

Comparison of the electrical characteristics of the solar cell for the system with and without reflector.

Incident angle	Reflector film						No-reflector film					
	I_{sc}	V_m	P_m	I_m	V_{oc}	FF	I_{sc}	V_m	P_m	I_m	V_{oc}	FF
0	0.522	0.298	0.134	0.449	0.408	0.629	0.399	0.365	0.128	0.350	0.473	0.678
10	0.520	0.316	0.139	0.441	0.425	0.632	0.472	0.340	0.140	0.413	0.461	0.645
20	0.524	0.328	0.148	0.450	0.443	0.635	0.470	0.340	0.139	0.408	0.455	0.649
30	0.526	0.328	0.149	0.453	0.443	0.638	0.468	0.340	0.141	0.414	0.461	0.653
40	0.516	0.316	0.144	0.457	0.473	0.591	0.443	0.353	0.137	0.388	0.473	0.653
50	0.511	0.328	0.146	0.446	0.455	0.630	0.363	0.365	0.118	0.324	0.473	0.687

operating solar cell temperature. The V_{oc} can be seen to be higher at higher incidence angles due to the lower temperature as can be seen in Fig. 25. However, it is important to evaluate the overall power production of the system to qualify the use of the reflective film for the system. Fig. 26 shows the maximum power produced under both the scenarios at different incident angles. It may be clearly seen that, the maximum power point for the case with the reflective film is higher at all the incidence angles. An average of about 6–7% increase can be expected by the use of the reflective film along the edges of the concentrator. The fill factor of the solar cell was found to drop considerably by the use of the reflective film as could be seen in Fig. 27.

From all the results presented in this section it may be seen that the temperature plays an important role in the overall power production of the system. Different temperatures and distributions are seen at different angles of incidence. However, it is clear that the use of reflective film does benefit the overall system output. The detailed variation of all the parameters is also shown in Table 2.

7. Conclusions

A dielectric based asymmetric concentrating photovoltaic system was analysed for its optical, electrical and thermal performance. Based on the losses shown by initial optical modelling, the impact of using a reflective film along its edges was explored both by modelling and experiments. Detailed analysis was carried out to showcase the changes in optical, electrical and thermal performance of the system. It could be seen that the illumination flux exiting the concentrator after using a reflective film increases

significantly. Also, a change in the position of the hotspots and the illumination peaks occurs. The peak value of the illumination intensity changes from 24 to 34 Suns. An average increase of 15.9% was seen in the overall power output while keeping constant temperature of 25 °C. However it's important to note that this illumination changes the operating solar cell temperature. To analyse the effect of such a change the electrical analysis solar cell is carried out by coupling it with the thermal analysis of the overall system. During the thermal analysis the solar cell was found to reach a temperature of 356–364 K for the case with the reflective film against a temperature range of 344–355 K for the case without the reflective film. Hence the temperature profiles obtained by the thermal analysis were used to analyse the electrical performance. It was found that the temperature has a parasitic effect on the overall performance of the system. Still, the addition of the reflective film was found to improve the performance by an average increase of 6% compared to the 15.9% predicted without including the thermal effects. In addition to this, the effects introduced due to the non-uniformity were also studied for the case with and without reflective film. In the case with no reflective film the average maximum power was found to drop 0.94% whereas in the case with reflective film the average drop was just 0.5%.

References

- [1] Brogren M, Wennerberg J, Kapper R, Karlsson B. Design of concentrating elements with CIS thin-film solar cells for façade integration. *Sol Energy Mater Sol Cells* 2003;75(3–4):567–75.
- [2] Chemisana D, Ibáñez M. Linear Fresnel concentrators for building integrated applications. *Energy Convers Manage* 2010;51(7):1476–80.

- [3] Mallick TK, Eames PC, Norton B. Non-concentrating and asymmetric compound parabolic concentrating building façade integrated photovoltaics: an experimental comparison. *Sol Energy* 2006;80(7):834–49.
- [4] Eames PC, Norton B. Detailed parametric analyses of heat transfer in CPC solar energy collectors. *Sol Energy* 1993;50(4):321–38.
- [5] Norton B, Kothdiwala AF, Eames PC. Effect of inclination on the performance of CPC solar energy collectors. *Renew Energy* 1994;5(1–4):357–67.
- [6] Baig H, Sellami N, Chemisana D, Rosell J, Mallick TK. Performance analysis of a dielectric based 3D building integrated concentrating photovoltaic system. *Sol Energy* 2014;103(0):525–40.
- [7] Mallick TK, Eames PC, Hyde TJ, Norton B. The design and experimental characterisation of an asymmetric compound parabolic photovoltaic concentrator for building façade integration in the UK. *Sol Energy* 2004;77(3): 319–27.
- [8] Mallick TK, Eames PC. Design and fabrication of low concentrating second generation PRIDE concentrator. *Sol Energy Mater Sol Cells* 2007;91(7): 597–608.
- [9] Baig H, Sarmah N, Heasman KC, Mallick TK. Numerical modelling and experimental validation of a low concentrating photovoltaic system. *Sol Energy Mater Sol Cells* 2013;113(0):201–19.
- [10] http://www.smooth-on.com/tb/files/CRYSTAL_CLEAR_200_TB.pdf.
- [11] Anon. Information about Dow corning brand silicone encapsulants. Midland, USA: Dow Corning; 2008.
- [12] Sarmah N, Richards BS, Mallick TK. Evaluation and optimization of the optical performance of low-concentrating dielectric compound parabolic concentrator using ray-tracing methods. *Appl Opt* 2011;50(19):3303–10.
- [13] Baig H, Heasman KC, Mallick TK. Non-uniform illumination in concentrating solar cells. *Renew Sustain Energy Rev* 2012;16(8):5890–909.
- [14] Chemisana D, Rosell JI. Electrical performance increase of concentrator solar cells under Gaussian temperature profiles. *Prog Photovolt Res Appl* 2013;21(4): 444–55.